

## Mineral Composite Assessment of Kerbala District in Iraq By Means of Remote Sensing

Amal M. Saleh

College of Agriculture /University of Baghdad

**Abstract:** Remote sensing is the science of acquiring, processing, and interpreting images and related data, acquired from aircraft and satellites, that record the interaction between matter and electromagnetic energy. In geologic terms Landsat provides data especially useful for mineral exploration. It can be used to identify areas containing minerals useful in the search for mineral deposits, including iron oxides and/or hydroxides (hematite, goethite, and limonite); clays (kaolinite, dickite, and montmorillonite); and carbonates (calcite, and dolomite). Utilizing remote sensing (RS) and geographic information systems (GIS) tools, mineral composite characteristics (heavy minerals, light minerals, and clay minerals) of Al-Hindiya in Iraq were investigated and mapped. Mineral composite (MC) index maps were produced from one LANDSAT-ETM+ satellite image taken in 2015 resulting by GIS. Employing bi-variety correlation analysis, relationships among index maps were investigated. According to the results, spatial distribution for heavy minerals maps indicated that the majority of the study area has Magnetite but poor Amphibole and Hematite. It is also observed that the sediments of the study area are composed essentially of Calcite and Gypsum; as dominant with Quartz. The results of spatial distribution for clay minerals maps showed that clay fraction is dominated by Kaolinite, mixed layer Illite\_Montmorillonite, and Montmorillonite\_Illite. Amphibole and Hematite index maps showed positive correlation. It is also observed that there was a positive correlation between Gypsum and Calcite index maps, while Quartz index map is negatively correlated with Gypsum index map. There were no significant correlations among clay minerals indicating that the clay minerals may be transported by Euphrates river and deposited as fluvial deposits.

**Keywords:** Remote sensing; ERDAS IMAGINE; Mineral composite; GIS; LANDSAT-ETM+; Index maps.

---

Date of Submission: 05-09-2017

Date of acceptance: 28-10-2017

---

### I. Introduction

Remote sensing can be understood as the science, technology and art of acquiring, processing, and interpreting airborne or spaceborne images that record the interaction between matter and electromagnetic energy (Aranoff, 2005). Nowadays a plethora of satellites surrounding the earth provides continuous sets of data of quite different nature used for navigation, positioning, meteorology, surface temperature, sea water condition, etc. Among the most interesting satellites dedicated to systematically provide global covered of earth resources are the Landsat family. In geologic terms Landsat provides data especially useful for mineral exploration. It can be used to identify areas containing minerals useful in the search for mineral deposits, including iron oxides and/or hydroxides (hematite, goethite, and limonite); clays (kaolinite, dickite, and montmorillonite); micas (illite, sericite, and muscovite); sulfates (jarosite, and alunite); and carbonates (calcite, and dolomite) (Corral et al., 2011).

On the other hand, Geologists can apply GIS in mining and mineral exploration to present data in an integrated platform by using traditional cross-sections and graphical strip logs in conjunction with planning map views. In mineral exploration geologists deal with various types and sources of data to explore for new economical mineral deposits. The data sources vary from geological maps, multispectral satellite images, hyper-spectral airborne and geophysical images to data in many formats. GIS is the best platform to bring all these data together in a geologist's computer and deliver fruitful outcomes. GIS can save money and decrease the regular cost to explore for minerals and this due to these reasons:

a) fewer hours spent digitizing to incorporate data into models; b) variety of GIS analysis methods on quantitative and raster data to look for anomalous areas; c) and the ability to capture old data of different types and view/analyze as compatible layers. Some of these data would only previously have been examined in paper formats (Al-Ramadan, 2012).

Utilizing remote sensing (RS) and geographic information systems (GIS) tools, mineral composite characteristics (ferrous minerals (FM), iron oxide (IO), and clay minerals (CM)) of the Kelkit

River Basin in Turkey were investigated and mapped (Dogan, 2009). Mineral composite (MC) index maps were produced from three LANDSAT-ETM+ satellite images taken in 2000. Resulting MC index maps were summarized in nine classes by using 'natural breaks' classification method in GIS. Using field data for which their geographic coordinates had been determined by global positioning system (GPS), developed MC maps were verified, and found dependable for environmental and ecological modeling studies (Dogan, 2009).

In Egypt, Tushka Lakes and the surrounding area were analyzed and mapped for land cover change and mineral composite (MC) characteristics, ferrous minerals (FM), iron oxides (IO), and clay minerals (CM) (Sarajlic, 2012). Land cover change and MC maps were developed using Landsat TM image and Landsat ETM+ image. Using ArcMap 10, developed MC index maps were classified into seven classes by using the natural breaks method. The developed maps from this study are to be used as a guide for agriculture and environmental decision making (Sarajlic, 2012).

Nowadays, there are many different techniques and many ready-to-use professional tools in form of software packages are available for researchers to help them perform the atmospheric correction of multispectral data (Khan, 2013).

This study has been aimed to develop updated thematic maps that reveal the spatial distribution of mineral composite of Kerbala District/Al-Hindiya:

- i. Heavy minerals (Amphibole, Hematite, and Magnetite).
- ii. Light minerals (Calcite, Gypsum, and Quartz).
- iii. Clay minerals (Illite, Montmorillonite, Kaolinite, and Montmorillonite-Illite).

The produced maps have the potential to help the decision makers and researchers who study in the region, and can be useful for the studies devoted to agriculture environment.

## II. Description Of The Study Area

Al-Hindiya or Hindiya is a city in Iraq on the Euphrates River. It is geographically situated on latitude 32° 17' 31.68" - 32° 47' 15.84" North and longitude 44° 17' 47.28" - 44° 05' 52.03" East. The city is located in the Kerbala District and it lies to the south of Baghdad and west of ancient Babylon (Fig.1a). The study area includes one main soil formation; the alluvial flood plain. The land is naturally vegetated with *Agool (Alhagi maurorum)*. The major soil families at this site is (fine, smectitic, active, calcareous, hyperthermic, Typic Torrifluvents) (Soil Survey Staff, 2014).

### 2.1. Climate

Al-Hindiya experiences a hot desert climate (Köppen-Geiger climate classification BWh) and the average maximum temperature is as high as 30.78°C (87.42 °F) (Peel et al., 2007). The district is at an altitude of about 30 metres (98 ft) above sea level (Sanlaville, 1989). Observations of rainfall at Hindiya gave a mean annual precipitation of 160 millimetres (6.3 in), but there were wide variances from a maximum of 568 millimetres (22.4 in) to a minimum of 37 millimetres (1.5 in) (Allan, 2001). In addition to the remarkable difference in the temperature between day and night, the wind prevalent in the area is mostly north west toward south east accompanied by sand storms especially in summer and sometimes winds come from the south and south west (Iraqi meteorological organization, 2008).

### 2.2. Stratigraphy of the study area

Sedimentary rocks of the Tertiary and Quaternary sediments are outcrops in Karbala District and include the followings from oldest to youngest:

- **Injana Formation (Upper Miocene):** The formation is exposed along both ridges of Tar Al-Najaf and Tar Al-Sayid, and in the eastern bank of Al-Razzaza Lake to the west of Karbala city. While in the rest of the areas it is either covered by Dibdibba Formation or thick layers of recent sediments.

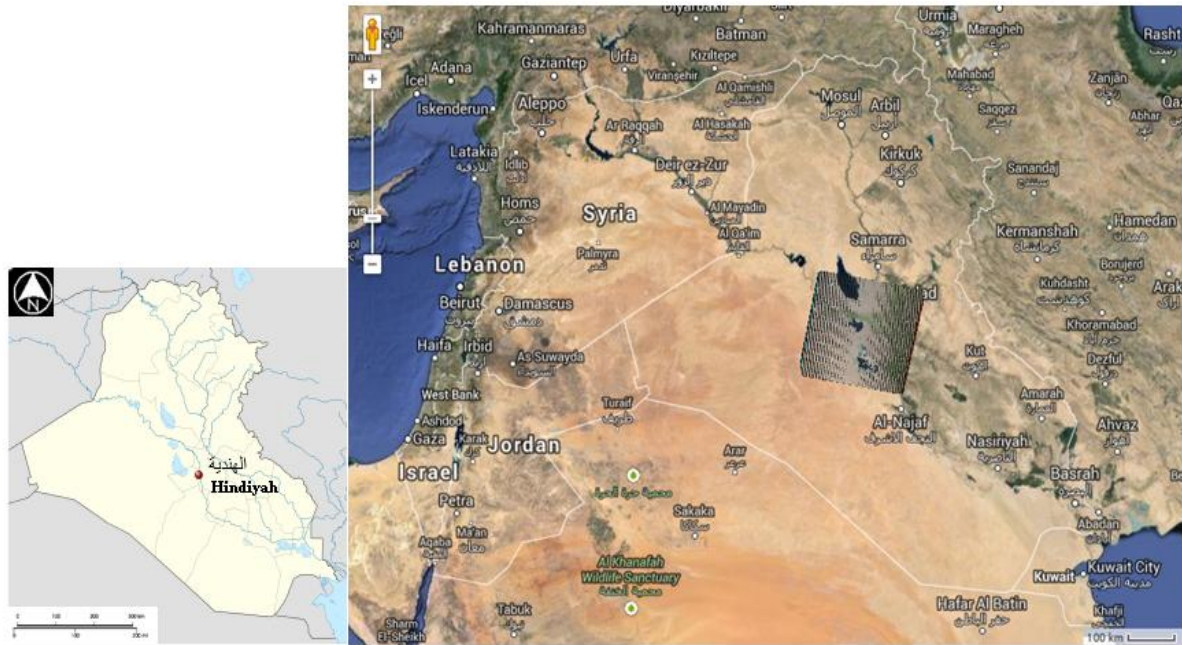


Figure 1.(a) Location map of the study area, (b) The Satellite Landsat ETM+scene.

- This formation is basically composed of sandstone and claystone with different colors (Green, grey, and brown). The contact between the Injana Formation and the Diddibba Formation appears as a soft layer of gravel. The environment of deposition varies from being marine to continental (Buday and Jassim, 1987).
- **Dibdibba Formation (Pliocene):** This formation is outcropped in the area between Al-Razzaza Lake and Karbala city from the northern west and west sides; it is mainly composed of sandstones, gravelly sandstones, and lenses of claystone. It forms a cover to Injana Formation deposits and the environment of deposition of this formation is continental (Buday and Jassim 1987). There is a gypcrete layer composed of sand, shale, gravel, and high percentage of gypsum are derived from the Quaternary sediments. Karbala represents a depocenter of the Dibdibba Formation along the Euphrates boundary fault (Jassim and Goff, 2006).
- **Quaternary sediments:** These sediments are outcrop inside Karbala city and extend to the Euphrates River and are composed of sand, shale, clay and there is gravel in some areas especially of Pleistocene sediments that exist in the northern part of the study area. The thickness of these sediments varies and increases toward the Euphrates River. The environment of deposition of these continental sediments is erosional and precipitational (Buday and Jassim, 1987).

Lithologically, the soils of Karbala was covered by Quaternary deposits during Holocene period; however, the Tertiary deposits were widely exposed in the area which mainly formed from depression fill deposits such as silt, sand, clay and almost with high gypsum content (Domas, 1983).

### III. Materials And Methods

One LANDSAT-ETM+ image detected on 30 September 2015 (path/row: 169/37) was downloaded free from Earth Explorer<sup>1</sup>. Geometric correction was tested by using 20 ground control points, and found accurate (root mean square (RMS) error <0.001) enough to proceed (Fig.1b). The stacked image was subset to obtain the area of interest (AOI) by using a vector AOI that was created from the map of Al-Hindiya. Then, a radiometric enhancement was applied on the subset image to remove effects of noise using image interpreter tool of ERDAS IMAGINE® software (2014) (Fig.2).

Spectral libraries are collections of reflectance spectra measured from materials of known composition, usually in the field or laboratory and spectra from libraries can guide spectral classification

<sup>1</sup>Earth Explorer is serviced by USGS: <http://edcns17.cr.usgs.gov/NewEarthExplorer/>

or define targets to use in spectral image analysis (Shippert, 2013). So, the next step involves the spectral analysis of multispectral Al-Hindiya imagery. ERDASIMAGINE® software (2014) contain spectral libraries developed by JPL (Jet Propulsion Laboratory), USGS, and Erdas which contain spectral signature for a wide variety of materials ranging from minerals, vegetation etc. These spectral libraries play a vital role in multispectral image analysis. For identification analysis of mineral composite, we adopted the approach of spectral signatures classification and identification (Target Detection Wizard-Project Specification). The subset image was used to create index maps of mineral composite by using spectral enhancement technique in ERDAS IMAGINE® software (2014) in order to bring out hidden and unclear land features. Created mineral composite (MC) index maps were converted to shape files in ArcGIS software (ESRI, 2008). Developed index maps were reclassified in ArcGIS using 'natural breaks' (Jenks) method (Fig.3, 4, 5) which are based on natural groupings inherent in the data and the features which are divided into classes whose boundaries are set where there are relatively big jumps in the data values (Dogan, 2009). After reclassifying, all indices were summarized in nine classes which are easy to interpret. 46 points were determined to extract corresponding index values in ArcGIS. Organizing extracted values as an XYZ file in Microsoft Excel software (Microsoft, 2010), bi-variety correlation analysis (Pearson coefficients) was conducted in SPSS 11 statistical software (SPSS, 2001).

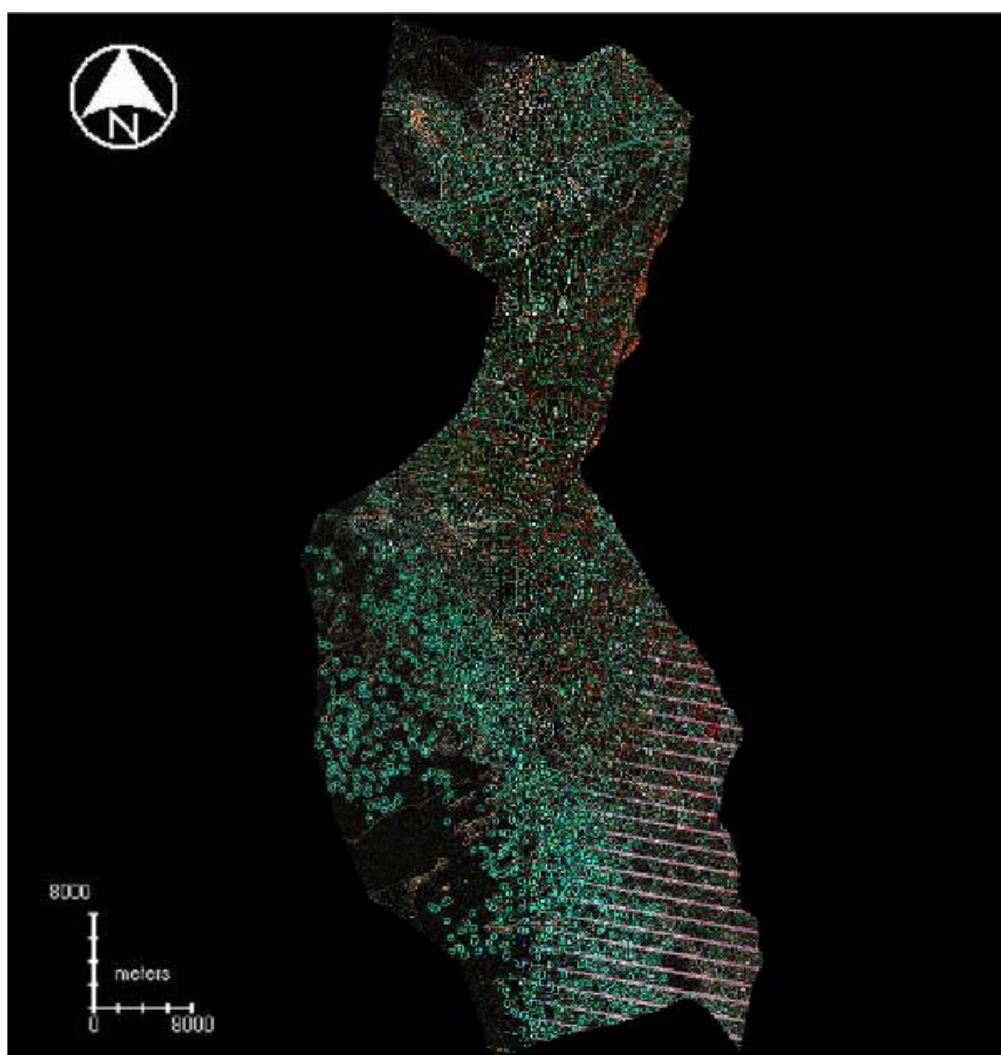


**Figure 2. Spatial \_ Enhancement image of Landsat ETM+data.**

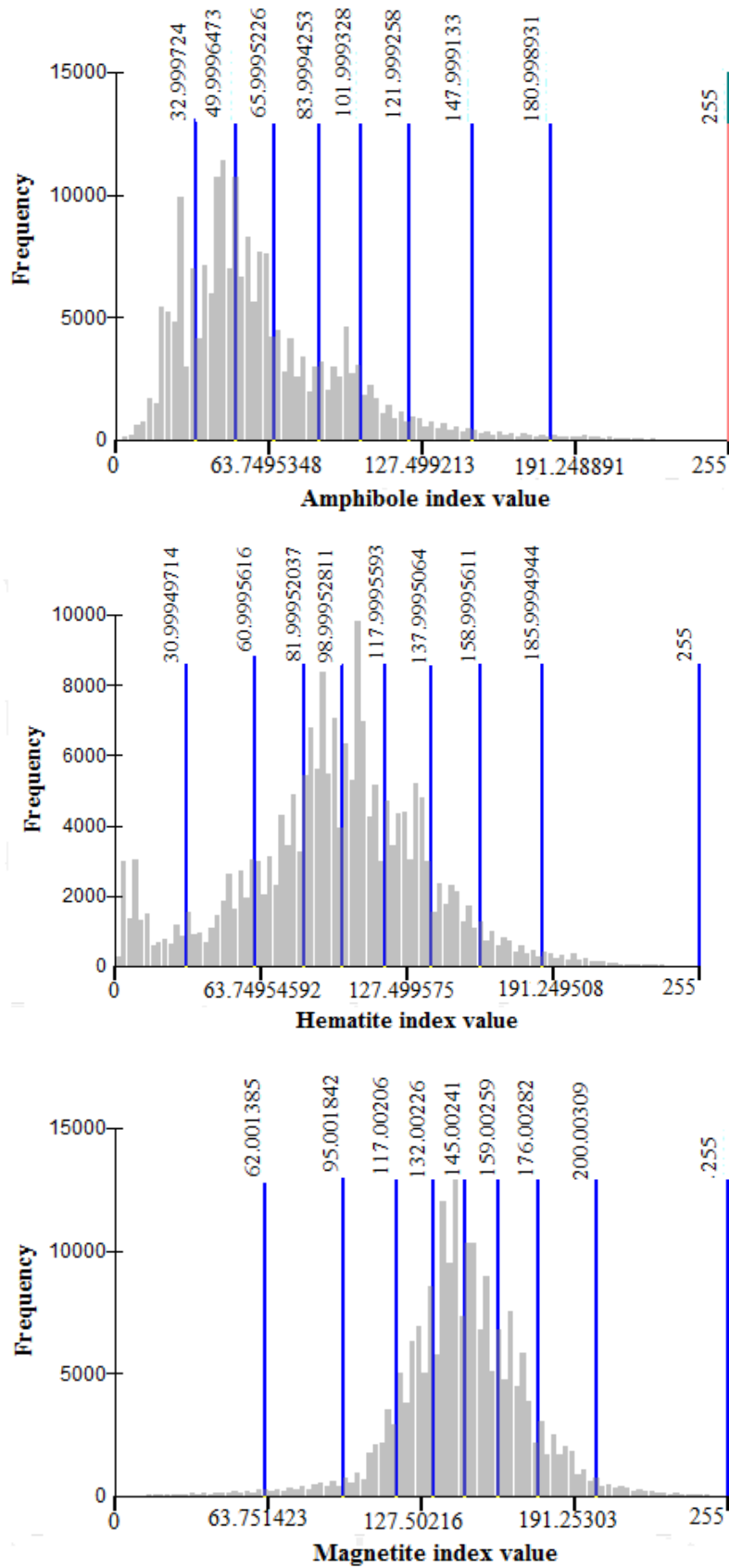


Figure 3. Histograms of Amphibole, Hematite, and Magnetite index maps.

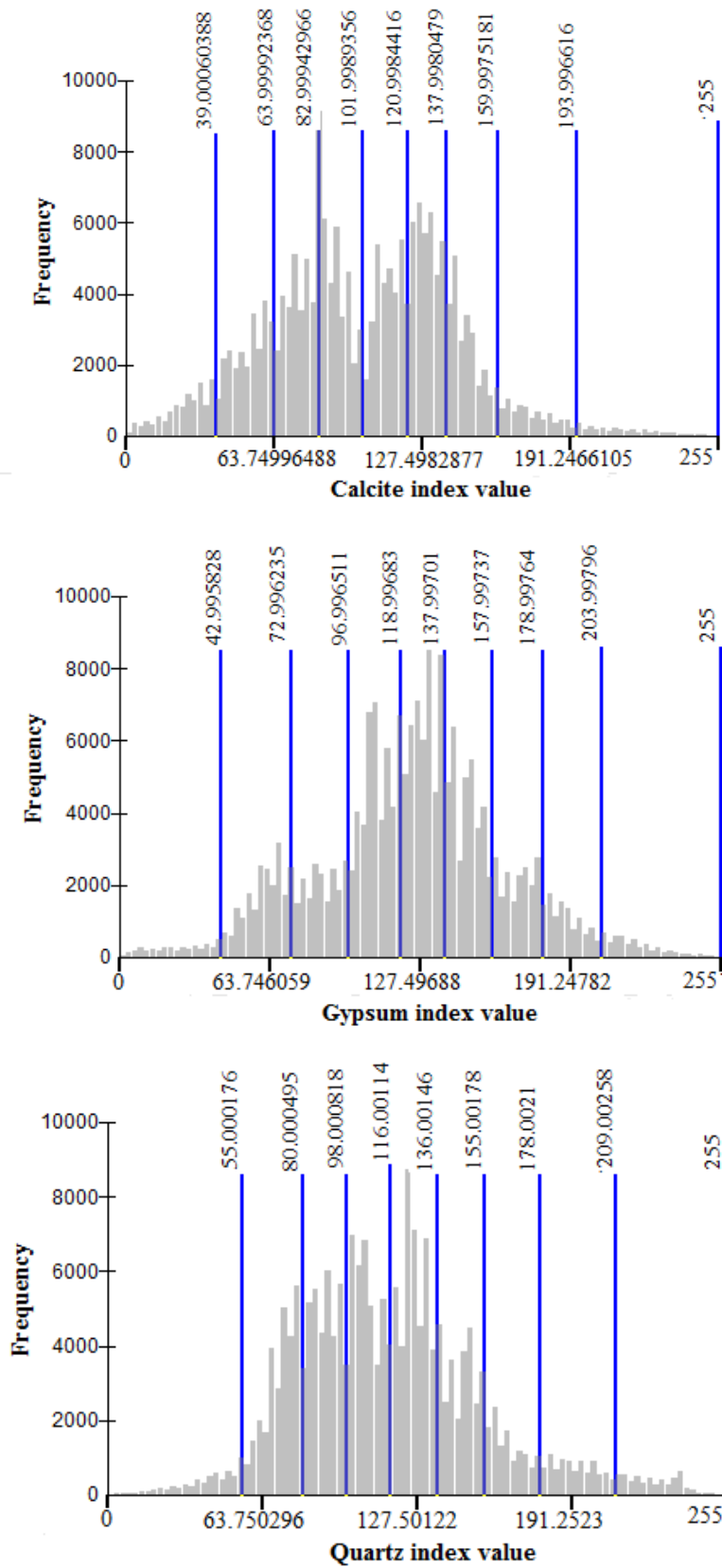


Figure 4. Histograms of Calcite, Gypsum, and Quartz index maps.

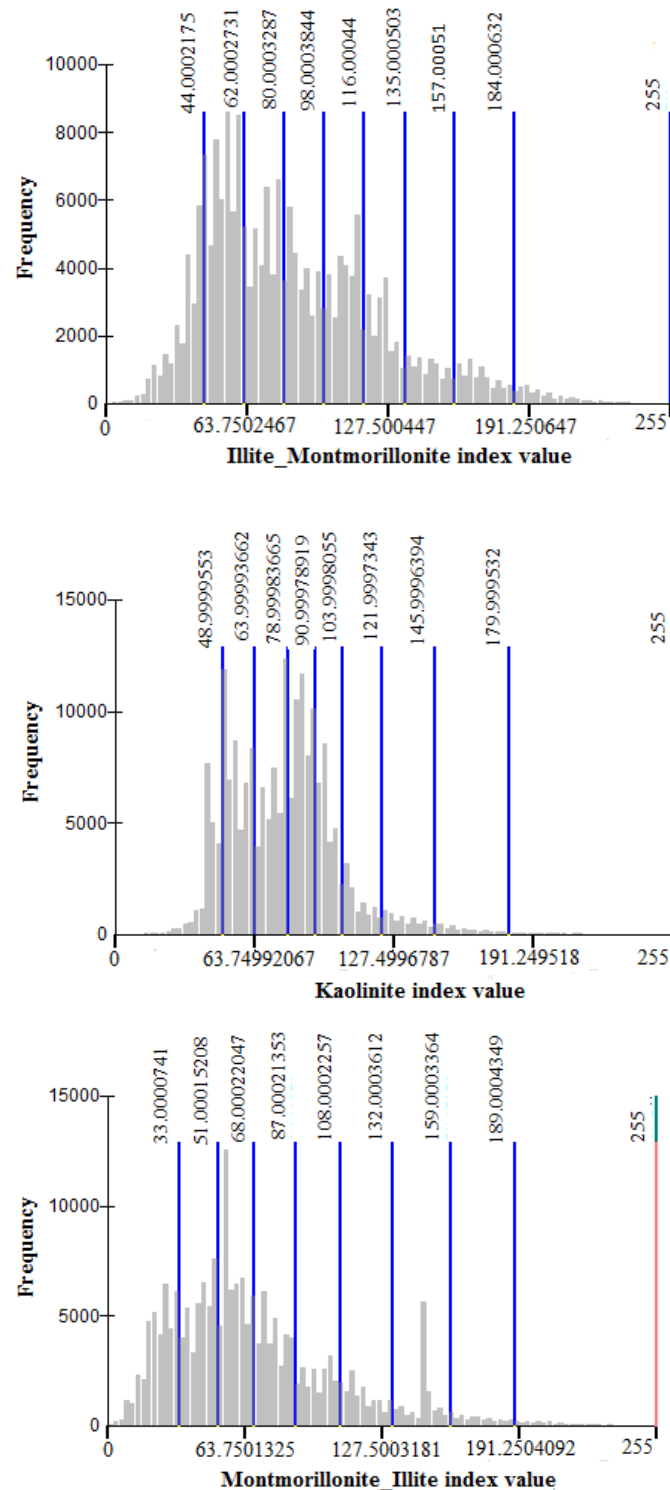


Figure 5. Histograms of Illite\_Montmorillonite, Kaolinite, and Montmorillonite\_Illite index maps.

#### IV. Results And Discussion

##### 4.1. Spatial distribution of Mineral composite (MC)

The minerals of Lower Mesopotamia soils could be categorized into two groups; non-clay minerals, and clay minerals. The first group comprises the heavy minerals assemblages comprises number of minerals; Amphibole, Hematite, and Magnetite. These minerals derived from igneous, metamorphic and even sedimentary rocks in the study area of Euphrates River (Al-Marsoumi and Al-Jabbri, 2007).

The second group comprises the light minerals composed of Calcite, Gypsum, and Quartz. The carbonates are originated from fragments of macrofauna shells (aragonite), and authigenic (as

microcrystalline Calcite) carbonate rock fragments (Albadran, 2006). Gypsum also occurs multisources were suggested for this mineral; authigenic by direct precipitation from ground water due to evaporation, some secondary gypsum has been blown from the gypsumiferous desert areas and deposited in Al-Hindiya soils under consideration (Buringh, 1960). Quartz forms the main light silicate minerals owing to its high resistance to erosion (Al-Marsoumi and Al-Jabbri, 2007).

The clay fractions of all the sediments have similar clay assemblages of Kaolinite. Kaolinite is a common mineral in Al-Hindiya soils, owing to Grim (1962), the presence of carbonate material in Al-Hindiya soils reflects the detrital origin of Kaolinite. Furthermore, illite, montmorillonite, and mixed-layered clay minerals were also detected; this phenomenon reflects an intermediate phase of illite and chlorite diagenetic alteration to montmorillonite (Al-Marsoumi and Al-Jabbri, 2007).

#### 4.1.1. Spatial distribution of heavy minerals

Spatial distribution of heavy minerals Amphibole, Hematite, and Magnetite classes were determined and given in Fig. 6, 7, 8. Nine index classes were interpreted under five categories namely, very rare (0-51); rare (51-102); medium (102-153); high (153-204); and very high (204-255) (Dogan, 2009).

Spatial distribution of Amphibole showed that nearly half of the District area (45.133%) participated in 'very rare' category, while the areas between 'very rare' and 'rare' categories covered (43.867%) of the total study area (Table 1). The areas that contain Amphibole in 'medium-high' category covered small portion (10.132%) of the total study area. The areas in 'high-very high' category covered minor portion (0.868 %) of the study area.

According to the spatial distribution of Hematite, The main part of the study area (50.940%) were assessed in 'very rare- rare' category, while the areas between 'rare' and 'medium' categories covered (36.822%) of the total study area (Table 1). The areas in 'medium-high' category covered small portion (10.695%) of the study area. The areas that contain Hematite in 'high-very high' category covered minor portion (1.543%) of the total study area.

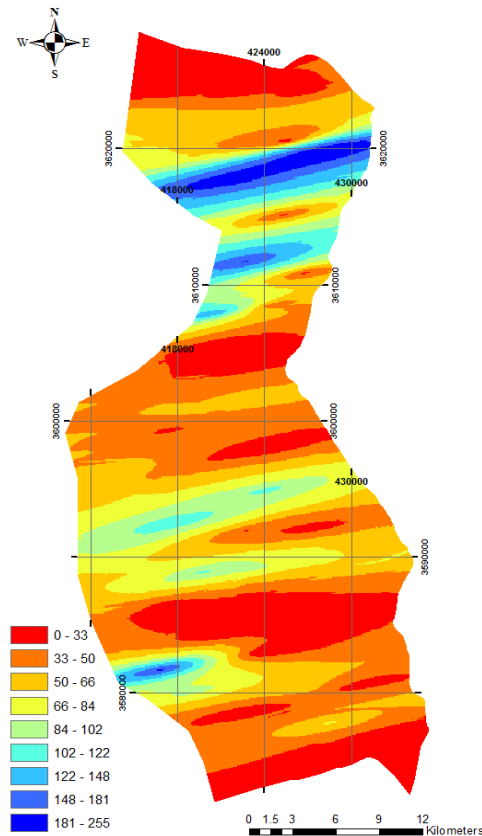


Figure 6. Amphibole index map of Al-Hindiya.



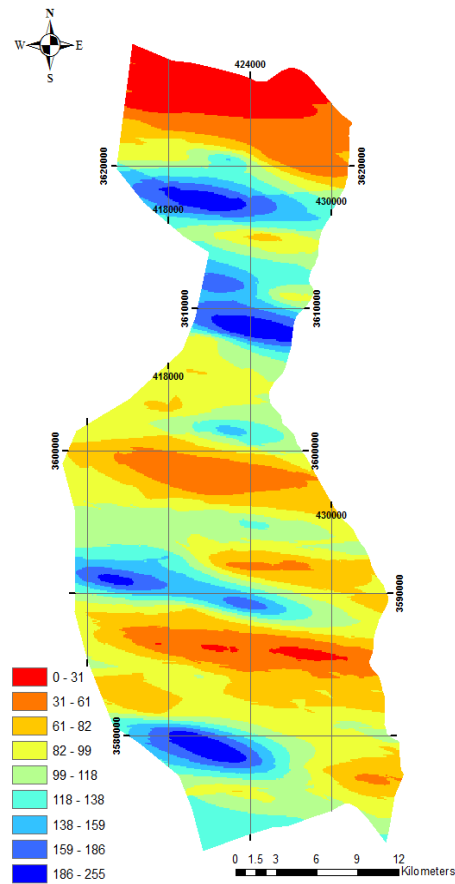


Figure 7. Hematite index map of Al-Hindiya.

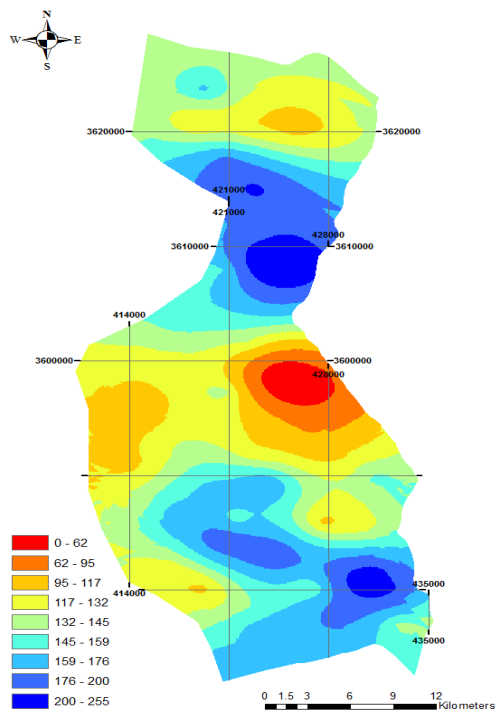


Figure 8. Magnetite index map of Al-Hindiya.

Table 1. Class cover areas of Amphibole, Hematite, and Magnetite in Al-Hindiya.

Class	Index values	Cover area km <sup>2</sup>	% of the study area	Interpretation	
				Category	% of the total study area
<b>Amphibole</b>					
1	0 - 33	270.724	18.979	Very rare	45.133
2	33 - 50	373.084	26.154		
3	50 - 66	314.821	22.070	Very rare - rare	22.070
4	66 - 84	161.193	11.300	Rare	21.797
5	84 - 102	149.732	10.497		
6	102 - 122	80.086	5.614	Medium	8.593
7	122 - 148	42.491	2.979	Medium - high	1.539
8	148 - 181	21.949	1.539		
9	181 - 255	12.377	0.868	High - very high	0.868
<b>Total</b>		<b>1426.457</b>	<b>100</b>		<b>100</b>
<b>Hematite</b>					
1	0 - 31	106.889	7.493	Very rare	7.493
2	31 - 61	137.461	9.637	Very rare - rare	9.637
3	61 - 82	195.125	13.679		
4	82 - 99	287.158	20.131	Rare	33.810
5	99 - 118	300.571	21.071	Rare - medium	21.071
6	118 - 138	224.676	15.751	Medium	15.751
7	138 - 159	104.008	7.291	Medium - high	7.291
8	159 - 186	48.556	3.404	High	3.404
9	186 - 255	22.013	1.543	High - very high	1.543
<b>Total</b>		<b>1426.457</b>	<b>100</b>		<b>100</b>
<b>Magnetite</b>					
1	0 - 62	15.194	1.065	Very rare - rare	1.065
2	62 - 95	33.213	2.328	Rare	2.328
3	95 - 117	101.507	7.116	Rare - medium	7.116
4	117 - 132	226.494	15.878	Medium	41.031
5	132 - 145	358.791	25.153		
6	145 - 159	314.011	22.013	Medium - high	22.013
7	159 - 176	236.341	16.569	High	24.440
8	176 - 200	112.278	7.871		
9	200 - 255	28.628	2.007	High - very high	2.007
<b>Total</b>		<b>1426.457</b>	<b>100</b>		<b>100</b>

In Magnetite point of view, the majority (94.600%) of the study area was evaluated between 'rare-medium' and 'medium-high' categories, and this was ensued by 'very rare-rare' (3.393%), and 'high-very high' (2.007%) categories, respectively (Table 1).

The results for heavy minerals maps indicated that the majority of the study area has Magnetite but poor Amphibole and Hematite. This indicates that the origin of sand dunes of Al-Hindiya is the recent sediments of the Euphrates river and the older nearby exposed geological formations (Mahmoud and Al-Ani, 1985).

The dust storms loads were depend on the direction of the wind and the geological formations that were in their path way. Consequently, the stable heavy minerals may reflect such geological formations as the regional dust storms blowing from western desert of Iraq (Al-Dabbas et al., 2011).

#### 4.1.2. Spatial distribution of light minerals

Spatial distribution of light minerals Calcite, Gypsum, and Quartz classes were determined and given in Fig. 9, 10, 11. Nine index classes were interpreted under five categories (Dogan, 2009). Spatial distribution of Calcite showed that (65.522%) of the District area participated in 'rare-medium' category, and this was ensued by 'very rare-rare' (17.094%), 'medium-high' (15.912%), and 'high-very high' (1.472%) categories, respectively (Table 2).

According to the spatial distribution of Gypsum, the main part of the study area (54.200%) was assessed in 'rare-medium' category, while the areas between 'medium' and 'high' categories covered (31.674%) of the total study area (Table 2). The areas that contain Gypsum in 'very rare-rare' category covered small portion (11.662%) of the study area. Minor portion (2.464%) of the study area was evaluated in 'very high' category.

In Quartz point of view, the majority (71.899%) of the study area was evaluated in 'rare-medium' category (Table 2). The areas between 'medium' and 'high' categories covered (18.413%) of the study area, while the areas in 'high-very high' category covered (7.093%) of the study area. The areas that contain Quartz in 'very rare-rare' category covered minor portion (2.595%) of the total study area.

The results for light minerals maps indicated that the sediments of the study area are composed essentially of Calcite and Gypsum; as dominant with quartz. These sediments reflect the relative rapid transportation of sediments by Euphrates river mainly during flooding phase (Al-Marsoumi and Al-Jabbri, 2007).

Gypsum and Calcium Carbonate minerals in Al-Hindiya soils are considered to be mainly of secondary origin (i.e., pedogenic), but some are of primary origin (i.e., geogenic) and are inherited from the parent material. Gypsum of pedogenic origin varies in shape, size, form, and distribution with soil depth. (Ataa and Muhaimed, 2007).

Quartz is the one of the most abundant minerals in Al-Hindiya, among the reasons for its abundance are:

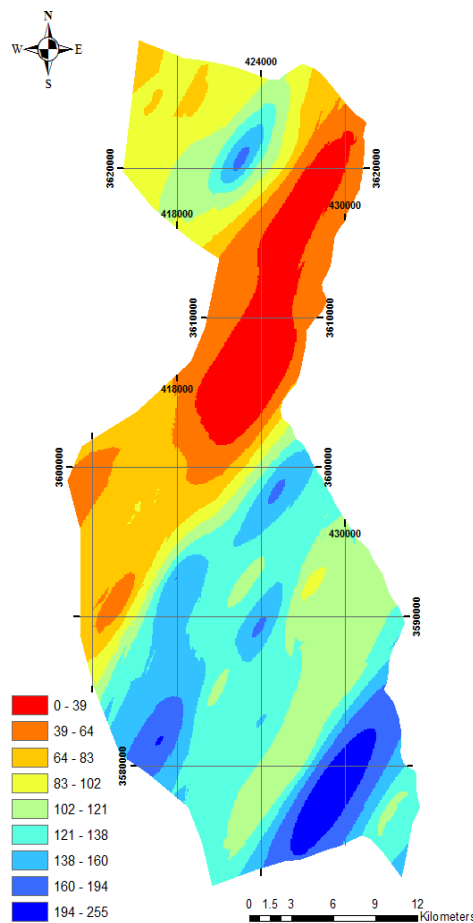


**Figure 9. Calcite index map of Al-Hindiya.**

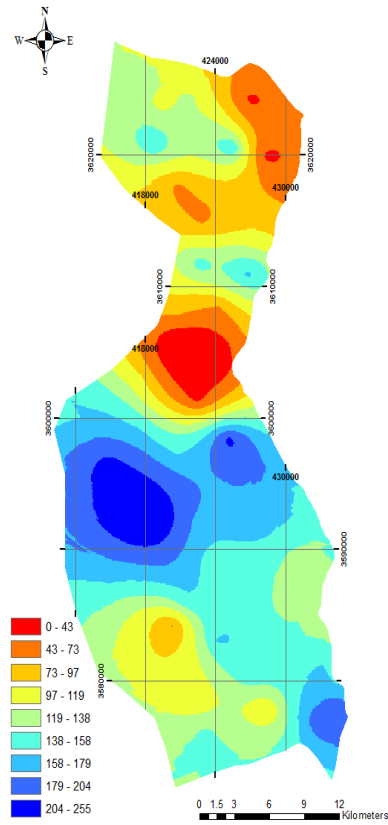


**Figure 10.**Gypsum index map of Al-Hindiya.

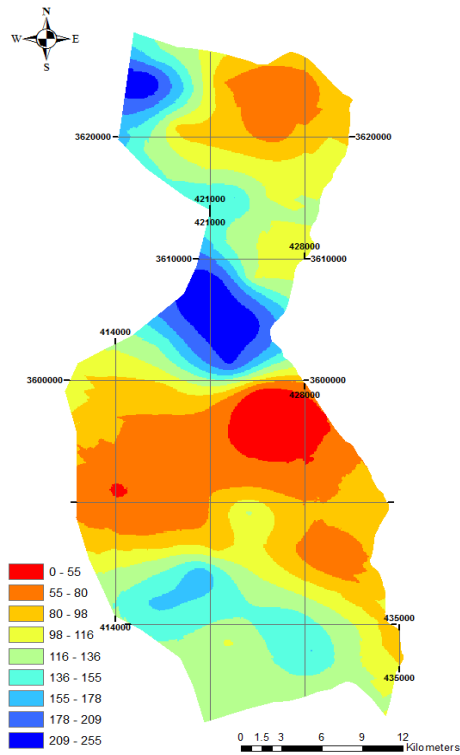


**Figure 11.**Quartz index map of Al-Hindiya.

Table 2. Class cover areas of Calcite, Gypsum, and Quartz in Al-Hindiya.

Class	Index values	Cover area km <sup>2</sup>	% of the study area	Interpretation	
				Category	% of the total study area
<b>Calcite</b>					
1	0 - 39	76.641	5.373	Very rare	5.373
2	39 - 64	167.202	11.721	Very rare - rare	11.721
3	64 - 83	243.991	17.105		
4	83 - 102	221.365	15.519	Rare	32.624
5	102 - 121	211.721	14.842		
6	121 - 138	257.559	18.056	Medium	32.898
7	138 - 160	167.216	11.722	Medium - high	11.722
8	160 - 194	59.763	4.190	High	4.190
9	194 - 255	20.999	1.472	High - very high	1.472
<b>Total</b>		<b>1426.457</b>	<b>100</b>		<b>100</b>
<b>Gypsum</b>					
1	0 - 43	27.183	1.906	Very rare	1.906
2	43 - 73	139.159	9.756	Very rare - rare	9.756
3	73 - 97	137.243	9.621	Rare	9.621
4	97 - 119	292.843	20.529	Rare - medium	20.529
5	119 - 138	343.069	24.050	Medium	24.050
6	138 - 158	246.154	17.256	Medium - high	17.256
7	158 - 179	126.380	8.860	High	14.418
8	179 - 204	79.276	5.558		
9	204 - 255	35.150	2.464	Very high	2.464
<b>Total</b>		<b>1426.457</b>	<b>100</b>		<b>100</b>
<b>Quartz</b>					
1	0 - 55	37.010	2.595	Very rare - rare	2.595
2	55 - 80	202.543	14.199	Rare	31.223
3	80 - 98	242.843	17.024		
4	98 - 116	263.877	18.499	Rare - medium	18.499
5	116 - 136	316.343	22.177	Medium	22.177
6	136 - 155	169.949	11.914	Medium - high	11.914
7	155 - 178	92.709	6.499	High	6.499
8	178 - 209	65.307	4.578	High - very high	4.578
9	209 - 255	35.876	2.515	Very high	2.515
<b>Total</b>		<b>1426.457</b>	<b>100</b>		<b>100</b>

- its stability in a wide pressure and temperature range.
- its chemical and physical resistance to weathering.

Quartz tends to accumulate in deposits of eroded material, both due to its physical and chemical resistance and because it is often formed from silicate minerals during chemical weathering (Driscoll, 2010).

#### 4.1.3. Spatial distribution of clay minerals

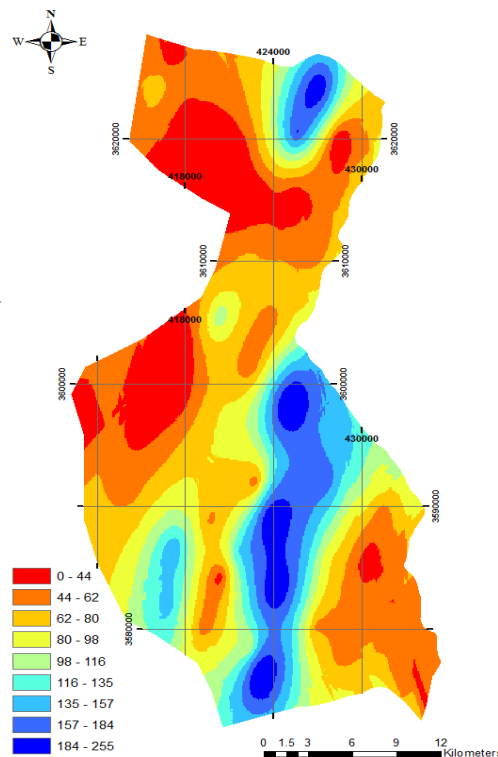
Spatial distribution of clay minerals Illite\_Montmorillonite, Kaolinite, and Montmorillonite\_Illite classes were determined and given in Fig. 12, 13, 14. Nine index classes were interpreted under five categories (Dogan, 2009).

According to the spatial distribution of Illite\_Montmorillonite, the main part of the study area (67.182%) was assessed in 'very rare-rare' category of the total study area (Table 3). The areas between 'rare' and 'medium' categories covered (22.033%) of the total study area, while the areas in 'medium-high' category covered small portion (8.850%) of the study area. The areas that contain Illite\_Montmorillonite in 'high-very high' category covered minor portion (1.935%) of the study area.

In Kaolinite point of view, the majority (73.918%) of the study area was evaluated in 'very rare-rare' category (Table 3). The areas between 'rare' and 'medium' categories covered (24.212%) of the study area, while the areas in 'medium-high' category covered very small part (1.456%) of the study area. The areas in 'high-very high' category covered minor portion (0.414%) of the study area.

Spatial distribution of Montmorillonite\_Illite showed that the main part of the study area (74.622%) was evaluated in 'very rare-rare' category, while the areas between 'rare' and 'medium' categories covered (16.137%) of the total study area (Table 3). The areas that contain Montmorillonite\_Illite in 'medium-high' category covered small portion (8.285%) of the study area. The areas between 'high' and 'very high' categories covered minor portion (0.956%) of the study area.

The results for clay minerals maps indicated that clay fraction is dominated by kaolinite, mixed layer Illite\_montmorillonite, and montmorillonite\_Illite in Al-Hindiya. The clay minerals may be transported by Euphrates river and deposited as fluvial deposits often bearing inherited properties from the weathered parent rock, so it is possible to use these minerals as tracers to elucidate the source area. Mixed layers of clay minerals are formed by the stacking of layers of different types or composition, and the diagenetic alteration processes are the main causes of increasing mixed layers (Meunier, 2005). Kaolinite can be formed by weathering of potash feldspar minerals (Grim, 1968) or as a result of re-erosion of ancient sediments (Al-Rawi, 1977), it may exist in the fluvial or coastal environments (Grim, 1968). The original source is either detrital coming from the high drainage channels or as a result from diagenetic processes during transportation by leaching of other minerals. The depositional environment of these minerals may be characterized by an arid to semi-arid climate in the source area (Al-Ali, 2010).



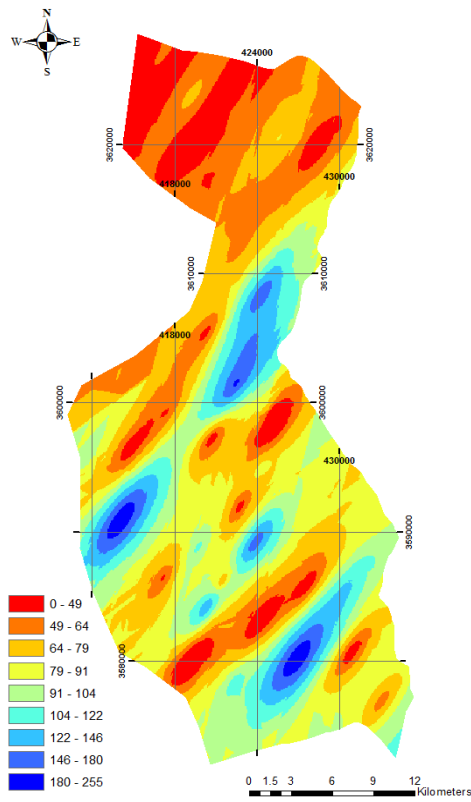


**Figure 13. Kaolinite index map of Al-Hindiya.**

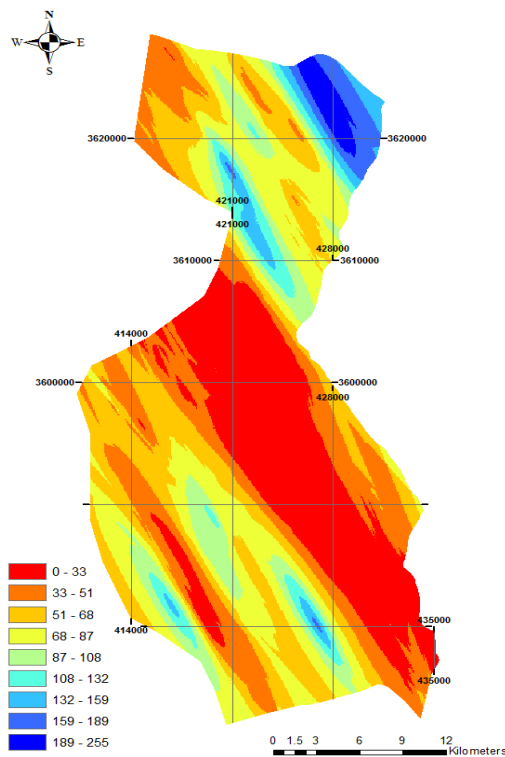


**Figure 14. Montmorillonite\_Illite index map of Al-Hindiya.**

Table 3. Class cover areas of Illite\_Montmorillonite, Kaolinite, and Montmorillonite\_Illite in Al-Hindiya.

Class	Index values	Cover area km <sup>2</sup>	% of the study area	Interpretation	
				Category	% of the total study area
<b>Illite_Montmorillonite</b>					
1	0 - 44	167.730	11.759	Very rare	11.759
2	44 - 62	351.402	24.635	Very rare - rare	24.635
3	62 - 80	245.083	17.181	Rare	30.788
4	80 - 98	194.104	13.607		
5	98 - 116	188.764	13.233	Rare - medium	13.233
6	116 - 135	125.535	8.800	Medium	8.800
7	135 - 157	66.399	4.655	Medium - high	4.655
8	157 - 184	59.834	4.195	High	4.195
9	184 - 255	27.606	1.935	High - very high	1.935
<b>Total</b>		<b>1426.457</b>	<b>100</b>		<b>100</b>

Class	Index values	Cover area km <sup>2</sup>	% of the study area	Interpretation	
				Category	% of the total study area
<b>Kaolinite</b>					
1	0 - 49	151.028	10.587	Very rare	10.587
2	49 - 64	318.027	22.295	Very rare - rare	22.295
3	64 - 79	283.805	19.896	Rare	41.036
4	79 - 91	301.557	21.14		
5	91 - 104	222.330	15.586	Rare - medium	15.586
6	104 - 122	78.120	5.476	Medium	8.626
7	122 - 146	44.921	3.15	Medium - high	1.456
8	146 - 180	20.766	1.456		
9	180 - 255	5.903	0.414	High - very high	0.414
<b>Total</b>		<b>1426.457</b>	<b>100</b>		<b>100</b>

Class	Index values	Cover area km <sup>2</sup>	% of the study area	Interpretation	
				Category	% of the total study area
<b>Montmorillonite_Illite</b>					
1	0 - 33	256.234	17.963	Very rare	36.636
2	33 - 51	266.364	18.673		
3	51 - 68	321.006	22.504	Rare	37.986
4	68 - 87	220.837	15.482		
5	87 - 108	137.081	9.610	Rare - medium	9.610
6	108 - 132	93.110	6.527	Medium	6.527
7	132 - 159	90.779	6.364	Medium - high	6.364
8	159 - 189	27.409	1.921	High	1.921
9	189 - 255	13.637	0.956	High - very high	0.956
<b>Total</b>		<b>1426.457</b>	<b>100</b>		<b>100</b>

4.2. Correlation coefficients of mineral composite (MC)

Correlation analysis results of 46 points delineated the relationships among produced raster maps of mineral composite (Table 4, 5, 6).

4.2.1. Correlation coefficients of heavy minerals

A positive correlation (0.370) was detected between Amphibole and Hematite variables at 0.05 level (2-tailed) emphasizing the relationship between these two variables (Table 4).



**Table 4. Pearson correlations of Amphibole, Hematite, and Magnetite indices.**

Index	Amphibole	Hematite	Magnetite
Amphibole	1		
Hematite	0.370*	1	
Magnetite	0.001	0.271	1

\*Correlation is significant at the 0.05 level (2-tailed).

The distribution of Fe<sub>2</sub>O<sub>3</sub> in floodplain sediment is related mainly to the geological substratum and mineralised areas, and particularly to areas with mafic and ultramafic rocks, and mineralisation. Iron is a major element in soil with a median value of 2.1% (Rose et al., 1979). It is present mostly as Fe<sup>2+</sup> in ferro-magnesian silicates, such as Olivine, Pyroxene, Amphibole and Biotite, and as Fe<sup>3+</sup> in iron oxides and hydroxides, as the result of weathering. It has both lithophile and chalcophile properties, forming several common minerals, including pyrite FeS<sub>2</sub>, magnetite Fe<sub>3</sub>O<sub>4</sub>, haematite Fe<sub>2</sub>O<sub>3</sub> and siderite FeCO<sub>3</sub>. It is also present in many rock-forming minerals, including Mica, Garnet, Amphibole, Pyroxene and Olivine.

**4.2.2. Correlation coefficients of light minerals**

Correlation analysis results between Gypsum and Calcite variables showed positive correlation (0.397) at 0.01 level (2-tailed) emphasizing the strong relationship between these two variables (Table 5).

**Table 5. Pearson correlations of Calcite, Gypsum, and Quartz indices.**

Index	Calcite	Gypsum	Quartz
Calcite	1		
Gypsum	0.397**	1	
Quartz	-0.156	-0.532**	1

\*\*Correlation is significant at the 0.01 level (2-tailed).

Different forms of sulfate minerals can be found in soils, with gypsum (CaSO<sub>4</sub>·2H<sub>2</sub>O) being the dominant type that occurs in central Iraq. The hot and dry climatic conditions are more suitable for the formation of gypsum than other forms of calcium sulfate minerals such as bassanite and anhydrite (Muhaimed et al., 2013).

Quartz variable negatively correlated with Gypsum (-0.532) at the 0.01 level (2-tailed) (Table 5). Quartz forms the main light silicate minerals owing to its high resistance to erosion. It is abundant in soils, mainly originating from physical weathering (fragmentation) of the parent material but also, by solution weathering, from carbonate parent materials (Martín-García et al., 2015). On the other hand Gypsum occurs in nature as a crystalline solid, and the solubility of Gypsum is impacted by many factors including particle size distribution, the amount of organic matter, the surface soil structure, the soil's moisture condition, and the timing and volume of rainfall (Amezketta et al., 2005).

**4.2.3. Correlation coefficients of clay minerals**

Correlation analysis results of clay minerals showed that there were no significant correlations among Illite\_Montmorillonite, Kaolinite, and Montmorillonite\_Illite (Table 6) indicating that the Lower Mesopotamian Plain was covered by a recent layer of flood material and in particular, irrigation sediment. This sediment has been deposited over very extensive areas as the result of an artificial process of sedimentation by a controlled irrigation system (Buringh, 1960).

**Table 6. Pearson correlations of Illite\_Montmorillonite, Kaolinite, and Montmorillonite\_Illite indices.**

Index	Illite_Montmorillonite	Kaolinite	Montmorillonite_Illite
Illite_Montmorillonite	1		
Kaolinite	-0.046	1	
Montmorillonite_Illite	-0.003	0.182	1

**V. Conclusions**

In this study, mineral composite raster maps of Al-Hindya were produced by using the RS and GIS tools. Consequently, the areas in rich and poor mineral composite content were determined with their cover size and geographical locations in a reliable and quicker way. We may generally conclude:

1. The results of spatial distribution for heavy minerals maps indicated that the majority of the study area has Magnetite but poor Amphibole and Hematite.
2. The results of spatial distribution for light minerals maps indicated that the sediments of the study area are composed essentially of Calcite and Gypsum, as dominant with Quartz.
3. The results of spatial distribution for clay minerals maps indicated that clay fraction is dominated by Kaolinite, mixed layer Illite-Montmorillonite, and Montmorillonite-Illite.
4. A positive correlation was detected between Amphibole and Hematite variables at 0.05 level (2-tailed) due to the distribution of Fe<sub>2</sub>O<sub>3</sub> in floodplain sediment related mainly to the geological substratum and mineralised areas.
5. Correlation analysis results between Gypsum and Calcite variables showed positive correlation at 0.01 level (2-tailed). This means that, calcium carbonate can be found in soils, with gypsum (CaSO<sub>4</sub>·2H<sub>2</sub>O) being the dominant type that occurs in central Iraq. A negative correlation between Quartz and Gypsum variables was found at 0.01 level (2-tailed). This result is related to the higher chemical and physical resistance of Quartz to weathering in comparison to the moderately soluble Gypsum.
6. There were no significant correlations among clay minerals indicating that the Lower Mesopotamian Plain was covered by a recent layer of flood material.

### References

- [1] Al-Ali, S. H. 2010. Geochemical and mineralogical study of the fluvial deposits at Abul Khasib area, south east of Iraq. *Mesopot. J. Mar. Sci.* 25(2): 154-165.
- [2] Albadran, B. 2006. Sedimentology and mineralogy of the Al-Hammar Marsh / Southern Iraq: A review. *Marsh Bulletin*, 1(1): 32-39.
- [3] Al-Dabbas M.; M. A. Abbas; and R. Al- Khafaji. 2011. The mineralogical and micro-organisms effects of regional dust storm over Middle East region. *International Journal of Water Resources and Arid Environments*, 1(2): 129-141.
- [4] Allan, T. 2001. *The Middle East Water Question: Hydropolitics and the Global Economy*. Publisher I.B.Tauris.
- [5] Al-Marsoumi, A. M. H.; and M. H. A. Al-Jabbri. 2007. Basrah Soils; Geochemical Aspects and Physical Properties- A Review. *Basrah Journal of Scienc.*, 25(1): 89-103.
- [6] Al-Ramadan, B. 2012. *Mineral Exploration Using GIS*. CRP 514: Introduction to GIS. City and Regional Planning Department, King Fahad University of Petroleum and Minerals.
- [7] Al-Rawi, I. K. 1977. Sedimentological study of the alluvial plain deposits in Diwania area. Unpublished M.Sc. Thesis, Baghdad University.
- [8] Amezketa, E.; R. Aragues; and R. Bazol. 2005. Efficiency of sulfuric acid, mined gypsum and two gypsum byproducts in soil crusting prevention and sodic soil reclamation. *Agronomy Journal*, 97: 983-989.
- [9] Aranoff, S. 2005. *Remote sensing for GIS managers*. ESRI Press, Redlands, California, 487 pp.
- [10] Ataa, R. M.; and A. S. Muhaimeed. 2007. Genesis of some gypsiferous soils in Iraq. *Al-Takani J.* 13:95-104.
- [11] Buday, T.; and S. Z., Jassim. 1987. *The regional geology of Iraq. Vol.2. Tectonism, Magmatism and Metamorphism*. GEOSURV. Baghdad. 352 pp.
- [12] Buringh, P. 1960. *Soils and soil conditions in Iraq*. Ministry of Agriculture, Baghdad, Iraq.
- [13] Corral, I.; F. González; A. Griera; M. Corbella; D. Gómez-Gras; and E. Cardellach. 2011. Landsat ETM+ Imaging for the Exploration of Epithermal Deposits in the Azuero Peninsula (Panama). *revista de la sociedad española de mineralogía, macla* n° 15.
- [14] Dogan, H. M. 2009. Mineral composite assessment of Kelkit River Basin in Turkey by means of remote sensing. *Journal of Earth Systems Science*, 118(6): 701-710.
- [15] Domas, J. 1983. *The Mesopotamian Plain Project/The Geology of Karbala-Kut-Ali Al-Gharbi area*. D.G. of Geological Survey and Mining, Rep. No.4.
- [16] Driscoll, K. 2010. Understanding quartz technology in early prehistoric Ireland. PhD thesis. UCD School of Archaeology, University College Dublin, Ireland. Scribd.com. Retrieved.
- [17] ERDAS. 2014. *ERDAS Field Guide*. Norcross, GA: Leica Geosystems GIS & Mapping, LLC.
- [18] ESRI. 2008. *ArcGIS 9.3, What is in ArcGIS 9.3*. (Environmental Systems Research Institute, Redlands, California, USA).
- [19] Grim, R. E. 1962. *Applied clay mineralogy*. McGraw-Hill Book Co. Inc., New York.
- [20] Grim, R. E. 1968. *Clay mineralogy*. 2<sup>nd</sup> Ed., McGraw-Hill Book Co., New York, 596 pp.
- [21] Iraqi meteorological organization. 2008. Climatic elements data of recorded in Karbala station for period from (1976 — 2007).
- [22] Jassim, S. Z.; and J. C., Goff. 2006. *Geology of Iraq*. Dolin, Prague and Moravian Museum, Brno, 341 pp.
- [23] Khan, J. 2013. Preliminary Results – Hyperspectral Image, Analysis for Dolomite Identification in Tarbela, Dam Region of Pakistan. *International Journal of Innovative Technology and Exploring Engineering*, 2(3): 30-34.
- [24] Mahmoud, M. M.; and R. A. Al-Ani. 1985. Heavy mineral analysis of sand dunes in the Western Desert of Iraq. *Jour. Geol. Soc. Iraq*, 18(1): 180-196.
- [25] Martín-García, J. M.; R. Márquez; G. Delgado; M. Sánchez-Marañón; and R. Delgado. 2015. Relationships between quartz weathering and soil type (Entisol, Inceptisol and Alfisol) in Sierra Nevada (southeast Spain). *European Journal of Soil Science*, 66: 179-193.
- [26] Meunier, A. 2005. *Clays*. Springer-Verlag, Berlin, Heidelberg, 472 pp.
- [27] Microsoft. 2010. *Microsoft Office Excel*. Microsoft Office Professional Edition (USA: Microsoft Corporation).
- [28] Muhaimeed, A. S.; S. R. al-Jeboory; K. A. Saliem; R. Burt; and J. V. Chiaretti. 2013. Genesis and classification of selected soils in an arid region of Central Iraq. A peer-reviewed contribution published in *Soil Horizons*, pp. 1-13.
- [29] Peel, M. C.; B. L. Finlayson; and T. A. McMahon. 2007. "Updated world map of the Köppen-Geiger climate classification". *Hydrol. Earth Syst. Sci.* 11: 1633-1644.

- [30] Rose, A. W.; H. E. Hawkes; and J. S. Webb. 1979. *Geochemistry in mineral exploration*. Academic Press, New York, N.Y., pp. 490-517.
- [31] Sanlaville, P. 1989. "considérations sur l'évolution de la basse mésopotamie au cours des derniers millénaires". *Paléorient* (in French) (Paléorient and CNRS Editions).
- [32] Sarajlic, S. 2012. Land cover change and mineral composite assessment of Tushka Depression, in Egypt, using remote sensing and GIS. Geology Graduate Student, Geosciences Department, Georgia State University.
- [33] Shippert, P. 2003. "Introduction to Hyperspectral Image Analysis". *Online Journal of Space Communication*, Ohio University, Athens, OH 45701, US online at <http://spacejournal.ohio.edu/pdf/shippert.pdf>, accessed 4 Jan 2013.
- [34] Soil Survey Staff. 2014. *Keys to soil taxonomy*. 11<sup>th</sup>.ed; 2014. USDA-Natural Resources Conservation Service.
- [35] SPSS. 2001. *SPSS 11.0 for Windows*. SPSS Inc., Chicago.

Amal M. Saleh. "Mineral Composite Assessment of Kerbala District in Iraq By Means of Remote Sensing." *IOSR Journal of Agriculture and Veterinary Science (IOSR-JAVS)*, vol. 10, no. 10, 2017, pp. 01–19.